Summertime Surges over the Gulf of California: Aspects of Their Climatology, Mean Structure, and Evolution from Radiosonde, NCEP Reanalysis, and Rainfall Data

MICHAEL W. DOUGLAS

National Severe Storms Laboratory, Norman, Oklahoma

JUAN CARLOS LEAL

Cooperative Institute for Mesoscale Meteorological Studies, University of Oklahoma, Norman, Oklahoma

(Manuscript received 9 January 2002, in final form 16 July 2002)

ABSTRACT

This paper describes aspects of summertime northward surges of low-level moisture over the Gulf of California, based on 9 yr (1980–88) of radiosonde observations and also from NCEP reanalyses. These events are usually referred to as ''gulf surges'' by forecasters in the southwestern United States. A composite structure of 38 well-marked surge passages at Empalme, Mexico, during this period is presented. Radiosonde observations were composited to obtain the synoptic-scale structure of the surge from 2 days before to 2 days after the surge passage at Empalme. The composites reveal that the surges, strongest in the lower troposphere, are associated with low-latitude cyclonic perturbations that pass south of the Gulf of California. The composite cyclonic perturbation associated with the surges can be traced back to the western Gulf of Mexico 2 days prior to surge passage at Empalme. Composites based on the NCEP reanalyses for the same dates also show a similar evolution, though with somewhat weaker amplitude. Rainfall data from Mexican stations along the eastern side of the Gulf of California show that the surges modulate the climatological daily rainfall totals by ~15%–30%. Finally, the evolution of surges appears to be related to the propagation of tropical storms over the eastern Pacific Ocean.

1. Introduction

Northward-propagating masses of relatively cool, moist air over the Gulf of California during the summer months are known as gulf surges (see Fig. 1 for geo- ?1 graphical terms used in this paper). Gulf surges were initially described in the early 1970s from routine surface and upper-air observations (Hales 1972; Brenner 1974). These case studies described particularly well-defined events that were followed by thunderstorm development in Arizona. The characteristics of these moisture surges that were observed at Yuma, Arizona, were that 1) the temperature decreased by 3°–5°C and the humidity and surface pressure increased over a period of less than 24 h, and 2) the surges were confined to below the 3 km level (~700 hPa), with greatest intensity near the surface.

?2 For a period of years little new information became available on gulf surges. The Southwest Area Monsoon Experiment (SWAMP) field program carried out during ?3 1990 (Reyes et al. 1994; Meitin et al. 1991) substantially increased the research interest in gulf surges, as several surges were observed by research aircraft and special sounding networks deployed during SWAMP. The datasets collected have led to descriptions of the mean southerly flow over the Gulf of California (Douglas 1995) and the simulation of surge events by mesoscale numerical weather prediction models (Stensrud et al. 1997; Anderson et al. 2000a). A second field program carried out in 1993 (described in Douglas and Li 1996) has similarly stimulated surge studies. A review of some of these and other studies can be found in Adams and Comrie (1997).

The early work of Hales (1972) and Brenner (1974) suggested that extensive cloudiness or tropical storms near the mouth of the Gulf of California might produce a northward flow of cooler maritime air that could appear as northward-propagating surges over the gulf. Very recent studies (Fuller and Stensrud 2000; Anderson et al. 2000a) have suggested that surges are related to either tropical storms south of Baja California, cyclonic perturbations (or tropical waves) propagating from the east, or the juxtaposition of these systems with extratropical troughs over the western United States.

Most studies of gulf surges have involved case studies, with those of recent years being a blend of observational and modeling activities. Studies attempting to determine the frequency of surges, or the average structure of these features, have been few. The study by

Corresponding author address: Michael W. Douglas, National Severe Storms Laboratory, 1313 Halley Circle, Norman, OK 73069.
E-mail: Michael.Douglas@nssl.noaa.gov

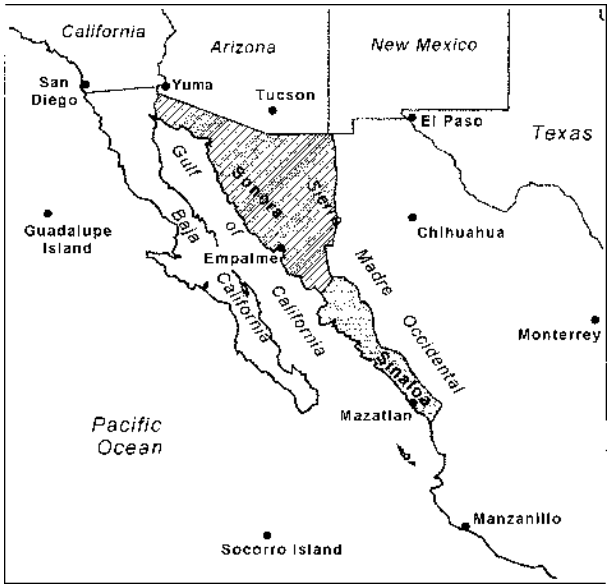

FIG. 1. Geography of the Gulf of California and surrounding region. Geographical terms mentioned in the text are shown; solid dots are radiosonde stations mentioned in text.

Anderson et al. (2000a) has examined the average structure of surges during 2-month-long periods when surge verification was feasible from SWAMP or other special observations. Their diagnosis of surge structure, divided into surges associated with tropical storms and surges associated with easterly waves propagating from over Mexico, was based on their simulations of the mesoscale flows over the Gulf of California region with a nested regional spectral model (Anderson et al. 2000b). This procedure was adopted to provide more detailed diagnosis of the surges and also to help identify the surge events, which are generally difficult to identify in routinely available analyses. However, since the surges in this study were identified from the simulation wind fields, the study was not strictly based on observations. Studies of the mean structure of surges relying primarily on observations are not evident in the literature.

Although strong surges are evident in the relatively good datasets from the 1990 and 1993 field programs, the number of surges is not sufficient to form solid generalizations or to construct reliable composites of their structure and evolution. To develop a more general description of surge events, and to identify the possible connection between surges and the larger-scale flow, a compositing procedure has been adopted in the present study. The general objective of the present work has been to describe the mean characteristics of gulf surges, including their evolution, based on analysis of historical radiosonde data and National Centers for Environmental Prediction (NCEP) reanalysis data. Specific objectives include 1) describing the evolution of the surge, 2) determining whether moisture fluxes associated with surges are a significant component of the overall summer moisture fluxes over the Gulf of California, 3) determining if rainfall is related to the surges, and 4) determining whether there is a link between tropical storms and hurricanes over the eastern Pacific and gulf surges.

This paper begins with an overview of methodology and data used, followed by a brief climatology of the moisture surges. A description of the vertical structure of the mean composite surge at the radiosonde site at Empalme, along the eastern shore of the central Gulf of California (see Fig. 1), is followed by a description of the synoptic-scale structure and evolution of the surge from both radiosonde and NCEP reanalysis data. Finally, we describe the relationship between surges and rainfall in northwestern Mexico, and an apparent connection between surges and tropical storms over the eastern Pacific.

2. Methodology and data

The basic methodology chosen for this study was to develop and employ a compositing procedure using radiosonde data to show the structure and evolution of the gulf surge throughout the troposphere. It was preferable to use original radiosonde data, rather than data from any particular gridded analysis, to eliminate the possibility that a systematic bias in a data assimilation scheme might affect the results. It was originally believed that the widely used NCEP reanalyses (Kalnay et al. 1996) would not have sufficient resolution to describe the surges in the lower troposphere, owing to inadequate resolution of the topography of the region. However, these reanalysis data proved to be valuable and have been used for a comparison with the radiosonde-based composites in section 5.

Before determining the average structure of gulf surges through a compositing procedure it was necessary to develop criteria to identify the dates of surge passage from available historical meteorological data. This was not a particularly simple task, as gulf surges do not have a universally accepted definition. The strongest evidence of a gulf surge passage is often a strong surface wind shift, from northwest (or weak southerly wind) to a strong south or southeast wind. Several factors complicate this simple criteria for defining surge events. First, outflow from isolated thunderstorms can show the same characteristics as surges, but may last for only a few hours. Second, there is a strong diurnal variation at virtually all sites around the gulf, associated with sea–land breezes, that can produce strong, diurnally varying wind shifts. Finally, of practical concern, the lack of surface stations around the Gulf of California that report hourly observations makes surge identification more difficult.

A clearer depiction of gulf surges can be made from radiosonde data. Field experiment data and routine observations at Empalme show that certain characteristics do tend to be associated with surge passages. These include 1) a decrease in temperature throughout the

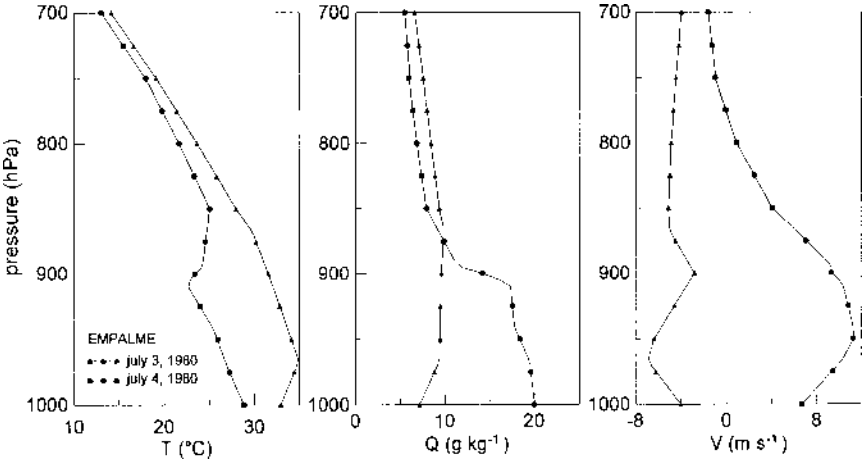

FIG. 2. Vertical profiles of (from left to right) (a) temperature, (b) specific humidity, and (c) meridional wind made before and after the passage of a strong gulf surge at Empalme between 3 and 4 Jul 1980. Observations were made at 1200 UTC.

boundary (well mixed) layer, 2) a deepening and moistening of the boundary layer, and 3) a wind shift from a northerly (or weak southerly) direction to a strong south wind component. Figure 2 shows a strong surge as it appears in the lower-tropospheric wind field and in radiosonde profiles at one site along the Gulf of California during the Experimento Meteorológico de Verano (Summer Meteorological Experiment) of 1993 (EMVER-93) field program.

There are several complications to the identification of gulf surges from radiosonde data. One problem is the small number of sites at which surges can be identified. Along the Gulf of California, radiosonde observations have been made routinely only at Empalme and Mazatlan. Mazatlan did not appear to show, from cursory examination, major temperature fluctuations associated with surges. Thus, surge identification generally rests on observations only from Empalme. Further, the observations from Empalme have not always been made twice daily, so the determination of the time of surge passage can be relatively coarse during these once-daily observing periods. Finally, even with twice-daily observations, the strong diurnal variation in the lower troposphere complicates surge identification, especially with weaker surges.

Due to the difficulties in working with the limited surface data, emphasis was placed on identifying surges with the available radiosonde data. The Empalme site, although being located only a few kilometers from the gulf, is subject to the development of a nocturnal boundary layer that tends to decouple the surface conditions from the atmosphere even a short distance above. Afternoon conditions are usually well mixed in the lowest few hundred meters, but are subject to a strong sea breeze. Thus, the surface observations do not always reflect the conditions over the gulf, or even over the coastal plain of Sonora. To minimize problems with identifying surges from soundings, and to produce a valid depiction of the conditions at other upper-air sites during surges at Empalme, a period of relatively complete radiosonde record during the summer season for the entire network was selected. This period was 1980–88, when Empalme made twice-daily observations. During the 1990s Empalme usually made once-daily observations and for several summers observations were very intermittent.

The radiosonde data were obtained from the National Oceanic and Atmospheric Administration/Forecast Systems Laboratory (NOAA/FSL) archive of historical radiosonde data for North America (available online at www.raob.fsl.gov). Both standard- and significant-level observations were used, and where necessary, data were interpolated to either 50- or 5-hPa vertical resolution for some display purposes. Because of the problems with varying periods of observation, only the period 1980–88 was used for this study. Further, as will be described in section 3, only observations from the months of July and August were used to provide a more homogeneous set of analyses.

As an example of the meteorological variations that are associated with gulf surges, the temperature, surface pressure, and integrated meridional moisture flux over the surface to 850-hPa layer at Empalme are shown in Fig. 3 for July 1980, the first month of the dataset used in this study. The shading in Fig. 3 corresponds to periods where the temperature decreases, the humidity increases, and the meridional wind intensifies in the lower levels of the atmosphere. A gradual increase in surface pressure is also evident, but with a marked diurnal variation. Collectively, these changes are similar to those commonly recognized as being associated with gulf surges.

Based on a general inspection of the characteristics of moisture surges that are evident from the time series at Empalme, a set of criteria were adopted to define objectively the occurrence of moisture surges at Em-

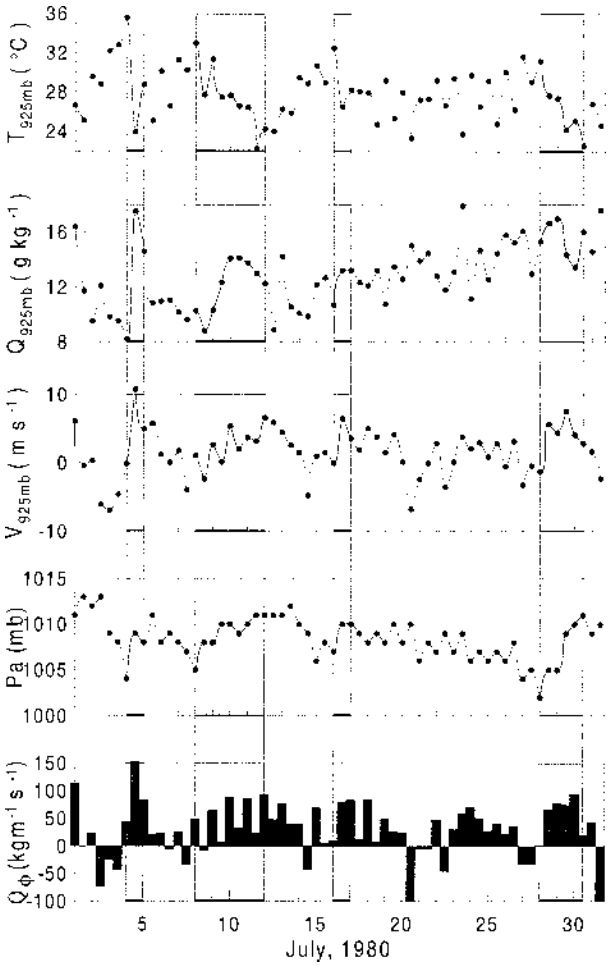

FIG. 3. Time series of (from top to bottom) 925-hPa temperature, 925-hPa specific humidity, 925-hPa meridional wind, surface pressure, and integrated meridional moisture flux over 1000–850 hPa layer at Empalme during Jul 1980 from twice-daily radiosonde data. The shaded vertical bands indicate periods of surge events.

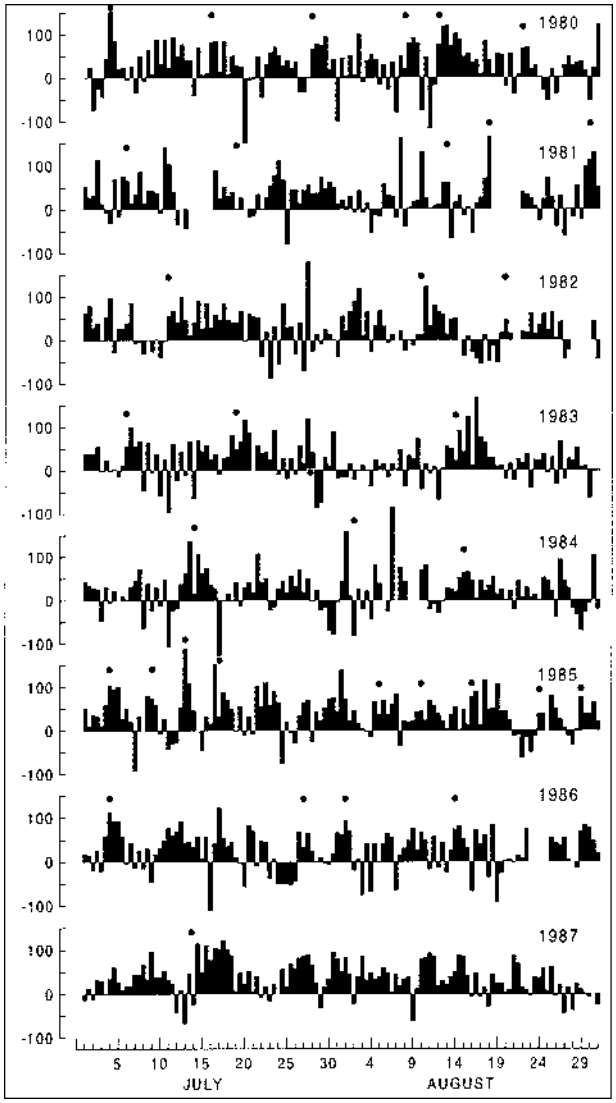

FIG. 4. Meridional moisture flux at Empalme, integrated from the surface to 850 hPa, for all observations made during the period Jul–Aug for the years from 1980 to 1987. The small black dots indicate the date of a surge passage at Empalme, as used in this study. The units for all plots is kg m^{-1} s^{-1}.

palme. The criteria chosen to indicate the passage of a moisture surge were 1) an increase in integrated surface to 850-hPa moisture transport of greater than 50 kg m^{-1} s^{-1}, 2) a decrease in temperature at 925 hPa of greater than 3°C, and 3) an increase in surface pressure of more than 3 hPa.

Although the above changes generally occurred over 24 h, some extended surges involved slower changes. Moisture surges were identified using these criteria during the summer months for the years used in this study. These results are discussed in section 3.

3. Climatology of moisture surges

Twice-daily radiosonde data from Empalme were examined for the months of July and August for the period 1980–88 to determine the variations, including synoptic and diurnal, of meteorological fields associated with moisture surges. The 925-hPa temperature, $T_{\phi 925\text{hpa}}$ (°C); the surface pressure, Pa (hPa); and the vertically integrated meridional moisture transport in the 1000–850-hPa layer, Q_ϕ (kg m^{-1} s^{-1}), were obtained.

Over the 9-yr period from 1980 to 1988, there are, according to our general criteria, an average of six moisture surges from July through August. On average, three surges occur in July and three in August. A similar frequency of surge events was seen by Fuller and Stensrud (2000), using 14 yr of surface wind and humidity data from Yuma, Arizona. Although the frequency is similar, we cannot exclude the possibility that some surges may originate north of Empalme, while others may not arrive as far north as Yuma. These are evident in the time series of meridional moisture flux (Fig. 4).

The surges show interannual variability, in agreement with Brenner's (1974) remarks.

4. Vertical structure of the moisture surges at Empalme

a. Compositing procedure

Despite the fact that moisture surges can differ in their intensity, depth, and duration, a compositing approach was employed to identify the mean characteristics of the surges at Empalme. To do this the original surges identified were subjected to further scrutiny and a subset of the stronger surges selected from the original dataset. Thirty-eight surges were identified from July and August Empalme observations that appeared to show similar characteristics in the evolution of the sounding profiles, as described above. In this compositing procedure day zero is considered that time when the surge effects are first noticed at Empalme. To make more data available for the composite, both 1200 and 0000 UTC data were used in generating the composites. A particular procedure was adopted to minimize the impact of the strong diurnal variation at Empalme. First, the data from 1200 UTC alone were used to identify the first sounding that showed postsurge conditions (cooler, southerly wind, higher surface pressure). This observation was considered day zero. The previous 1200 UTC observation was considered day T_{0-1} and the following 1200 UTC observation as day T_{0+1} etc. Then, exactly the same procedure was used with the 0000 UTC observations. Then the climatological mean profiles of temperature, wind, and humidity were calculated from the 9 yr of July and August observations at Empalme. The surge mean profiles were subtracted from the climatological mean profiles to obtain profiles showing the anomaly of the surge conditions with respect to ''climatology'' for both the 1200 and 0000 UTC observation times. These anomaly profiles were then averaged together to obtain one anomaly profile for each day.

The compositing procedure naturally tends to blur the time of the surge onset. In essence, the anomaly surge profiles are an average of both 1200 and 0000 UTC profiles and, since the same surge events are used, the day zero observations can occur anywhere from 0 to 24 h after the actual time of a surge passage. However, this is the same as if only one synoptic time's data were used, and we gain the benefit of using both daily observations, to strengthen the signal–noise ratio.

During the course of this work, composites based only on 1200 UTC and only on 0000 UTC data were generated. These showed essentially the same results as the 0000 + 1200 UTC mean composites that will be discussed below. In addition, composites of the structure and evolution of surges were examined using only July or only August data—they were virtually identical. Finally, surges from the periods 1980–84 and 1985–88 were composited separately, and again the differences were minor. These results lend confidence to the significance of the final results.

b. Results

The changes associated with the gulf surge passage at Empalme are presented here in several forms. First are time–pressure sections of the profiles of temperature, humidity, and wind, followed by profiles of their anomaly with respect to climatology and then plots of the sounding profiles.

Time–pressure sections of temperature show that the highest temperature occurs 1 day before the surge passage (Fig. 5a) coincident with an increase in specific humidity (Fig. 5b). The changes are much smaller above 800 hPa. The wind changes associated with the surge are also abrupt (Fig. 5c), and are most apparent between 950 and 900 hPa. The wind shift decreases rapidly above this level, becoming negligible by 700 hPa. This shallow vertical extent to the surges is similar to both observational (Douglas 1995) and observational/modeling findings of Stensrud et al. (1997) based on SWAMP experiment data (Meitin et al. 1991). The surface wind change is noticeably smaller than at 950 hPa, presumably because of the effect of surface friction on reducing the overall winds at this level. Figure 5d shows that the changes in the horizontal moisture flux vectors during the surge passage are similar to the wind changes, but even more abrupt, since the wind shift is amplified by the moisture increase during the surge passage. What is especially evident from Fig. 5d is that the horizontal moisture flux is very small at 500 hPa, and that changes during the surge are significant only between the surface and about 800 hPa.

The relatively small changes evident in both temperature and dewpoint sections (Figs. 5a,b) very near the surface reflect the presence of the Gulf of California, only 3 km away, that tends to dampen near-surface fluctuations of both humidity and temperature. These smaller changes in the surface temperature and humidity illustrate the difficulty of identifying surges from surface data alone, and argues for using the Empalme sounding data to identify the surge passages.

Some features are better shown from time–pressure sections of anomalies of the various quantities from their climatological mean (Fig. 6). Figure 6a reveals that the largest temperature anomaly is the warm anomaly prior to the surge passage. Its magnitude substantially exceeds that of the cold anomaly after surge passage ($+2.5^\circ$ versus -1°C). The warm anomaly also has a larger amplitude at higher levels than does the cold anomaly. The average temperature decrease, of about 3.5°C between the presurge and day-of-surge soundings at 950 hPa, is less than some individual surges, which have shown changes of 7°C (Fig. 2). The compositing procedure has undoubtedly reduced the amplitude of the variations, in both time and in the vertical.

The moisture anomaly section (Fig. 6b) shows that

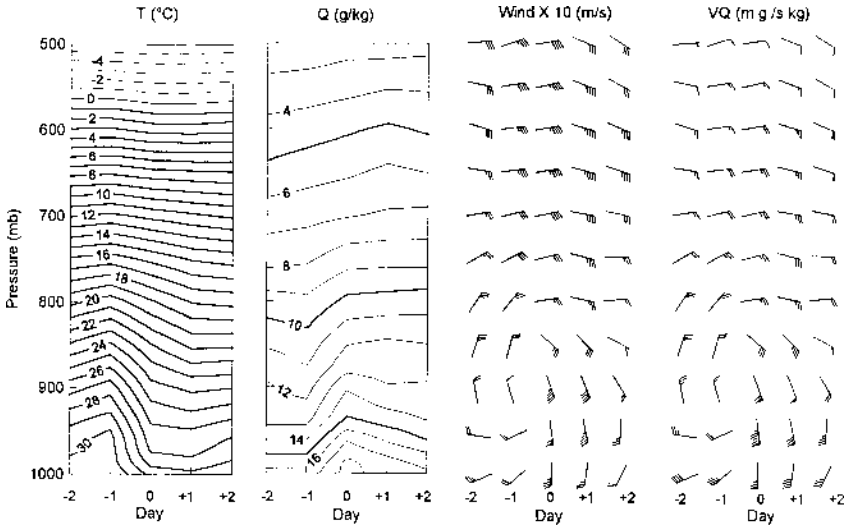

FIG. 5. Time–pressure sections of the (a) temperature, (b) specific humidity, (c) wind, and (d) moisture flux at Empalme during the composite surge passage. Winds are plotted to enhance the signal; full barb is 1 m s^{-1}, half barb is 0.5 m s^{-1}. Contour interval for temperature is 1°C; for specific humidity it is 1 gm kg^{-1}. For moisture flux one barb equals 10 m g s^{-1} kg^{-1}; a flag is 50 m g s^{-1} kg^{-1}.

the q anomalies are concentrated closer to the surface than the temperature anomalies, and only small changes occur above 900 hPa. One interesting feature is that at day T_{0+2} the near-surface moisture is near normal, while there is a positive anomaly near 850–800 hPa. As with the temperature anomaly, the moisture anomaly appears to slope upward with time.

The anomaly time sections of wind and moisture flux (Figs. 6c,d) are qualitatively similar to their original sections in Fig. 5, but are more symmetric about the surge onset date. Although the largest wind anomaly is found at 950 hPa on the surge day, the northerly wind anomalies are nearly as large over a deep layer (950–850 hPa) 2 days prior to surge passage. The wind changes appear to be smallest near 750 hPa, with larger changes both below and above this level. The anomaly moisture flux section (Fig. 6d) shows the expected result of small changes above 800 hPa. Interestingly, it is not obvious from the anomaly time–pressure section that the surge effects a net northward moisture flux, since the presurge southward anomaly flux appears to nearly balance the postsurge northward flux. The monthly or seasonal mean moisture transport is, however, clearly northward from Fig. 4.

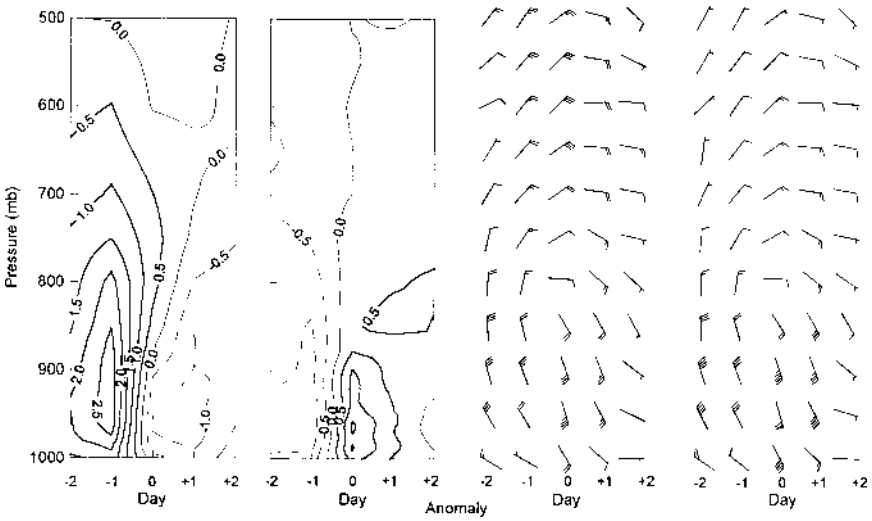

FIG. 6. Same as in Fig. 5 except all figures are anomalies from the Jul–Aug climatological profiles, and contour intervals are 0.5°C for temperature and 0.5 gm kg^{-1} for specific humidity. Positive contours are solid; negative contours are dashed.

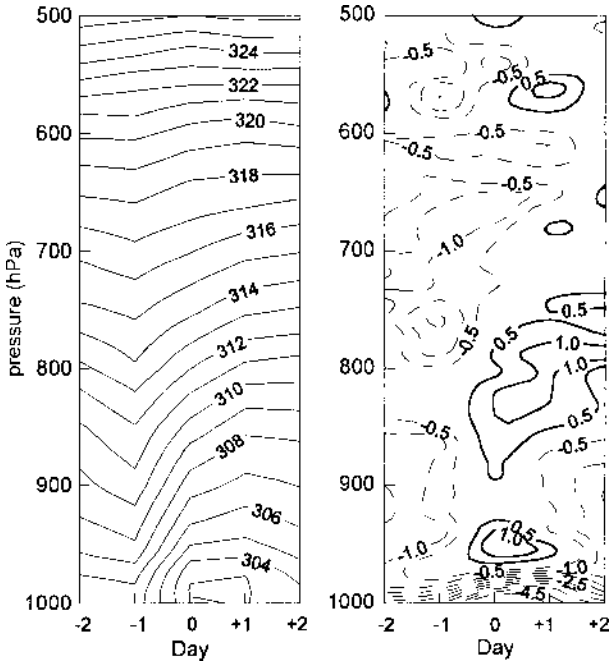

FIG. 7. Same as in Fig. 6 except showing (a) potential temperature (K) and (b) anomaly of static stability (contours are every 0.5×10^{-3} °C hPa^{-1}; see text) from the long-term Jul–Aug mean. In (b) no zero contour is plotted for clarity. Positive stability contours are solid; negative anomalies are dashed.

A time section of potential temperature (θ) (Fig. 7a) shows some features of the surge that are not as apparent from the temperature anomaly section. The isentropes slope upward along the surge boundary, similar to cold frontal structures (Djuric 1994, p. 189). A simple measure of static stability,

$$(\Delta\theta/\Delta P) \times 100,$$

was calculated from the θ values in Fig. 7a with a ΔP of 10 hPa, and with a Hanning smoother (Press et al. 1986) applied to the θ values to minimize small-scale noise. The factor of 100 was chosen to display the contours more legibly in Fig. 7b, which shows anomalies from the July–August mean values. The most obvious feature is the region of enhanced stability after surge passage, between 950 and 750 hPa, that slopes upward with time. This is associated with the stable layer capping the surge. The stability prior to the surge arrival is less than normal, including on the day of the surge at higher levels (~700 hPa). This reflects the northwesterly winds (Fig. 5c) that are advecting warm, less stable air from the northwestern deserts of Sonora or the southwestern United States. Presumably this air has been destabilized (brought closer to the dry-adiabatic lapse rate) by successive cycles of diurnal heating over the deserts of northwestern Mexico and the southwestern United States.

c. Surge signals at nearby stations

The question naturally arises as to whether surge signals are evident at other stations besides Empalme. Figure 8 shows that other stations do reflect the surge. Mazatlan, the radiosonde station at the southern end of the Gulf of California, shows a rather strong wind shift 1 day prior to that at Empalme. The magnitude of this shift at 950 hPa is ~30% of the wind shift magnitude at Empalme, but this changes with height. The change appears similar to Empalme at 800 hPa but is more pronounced than Empalme by 500 hPa. The most apparent difference between the Empalme and Mazatlan plots is the lack of a significant temperature anomaly at lower levels associated with the wind shift at Mazatlan. Only a weak warm and cool anomaly couplet is evident, and this appears to have its greatest amplitude near 700 hPa. This contrasts with the clear warm and cool anomalies at low levels apparent at Empalme. Socorro Island, far to the southwest of Mazatlan, shows a warm anomaly similar to that at Mazatlan, but slightly lower down. A corresponding cool anomaly after the surge passage is not apparent. This lack of a cool anomaly might be simply a result of the considerable distance from the Gulf of California, or a limitation of the compositing procedure, which ended at 2 days after the surge passage at Empalme. Of interest at Socorro is the relatively broad (in time) and vertically extensive warm anomaly in the middle and upper troposphere. This is a characteristic of the structure of tropical depressions and storms, which have warm cores at higher levels associated with extensive convective activity (Anthes 1982).

5. Synoptic-scale structure and evolution of the surge

It is possible to describe the three-dimensional structure of a gulf surge together with its evolution by compositing radiosonde observations from surrounding stations with respect to the date of surge passage at Empalme. By using the same dates used to prepare Fig. 5 the horizontal structure of the surge at different levels has been described from 2 days before to 2 days after the surge passage at Empalme. Characteristics of the surface pressure field associated with surge passages, using both observations and NCEP reanalyses, are presented in section 5a. The evolution and structure of the wind, temperature, and moisture fields from radiosonde observations are discussed in section 5b. In section 5c we describe the upper-air surge structure and evolution using NCEP reanalysis data.

The presentation in this section is done in terms of anomalies from the mean July/August conditions—a mean determined for the period 1980–88. This is done to compare the structure and amplitude of the surge at different levels and over different regions, where the varying mean state might otherwise tend to mask the geographical structure of the surge.

a. Surface pressure evolution during the surge

Surface pressure information from the radiosonde stations allows for an estimate of the surge evolution and

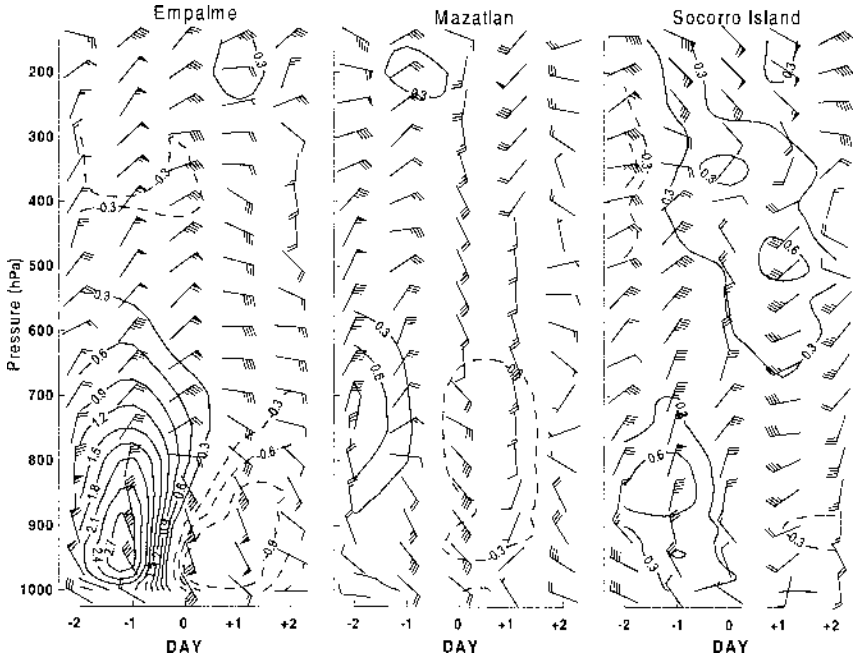

FIG. 8. Comparison of the changes in temperature and wind evident at Empalme and two other radiosonde stations near the southern Gulf of California. Plotting convention of winds is flag is 2.5 m s^{-1}, full barb is 0.5 m s^{-1}, and contour interval of temperature anomaly from the Jul–Aug mean is 0.3°C (negative anomalies dashed).

intensity that is independent of the radiosonde sensors themselves. However, because the reported surface (not sea level) pressure from a station may have significant systematic errors associated with incorrect calibration of the station's barometer, we have applied a simple procedure to analyze the pressure anomaly. The mean surface pressures were first calculated at each synoptic time from all of the July and August radiosonde observations for the 9-yr period. Then these mean station pressures were subtracted from the average of the station pressures during each of the days of the composite surge evolution. Thus an anomaly was obtained independent of whatever systematic station pressure error might exist. A similar procedure was applied to the daily NCEP reanalysis surface pressure data. Both sets of analyses (direct observation based and NCEP reanalysis based) were quite similar; hence, we discuss the evolution from the NCEP-reanalysis-based composites, while the amplitude of the surge event can be seen convincingly from the observation-based composite.

The NCEP-reanalysis-based surface pressure anomaly composites (Fig. 9) show that an elongated low pressure anomaly is located between Empalme and Mazatlan 1 day before the surge arrival. On the day of the surge this anomaly has extended northwestward, to between Empalme and San Diego. The northwestward movement of the anomalies is apparent, as is the replacement of the negative anomalies prior to the surge with positive anomalies after surge passage. This along-gulf variation in surface pressure gradient was also seen in the SWAMP surges (Stensrud et al. 1997). What is perhaps surprising is that there are major changes west of the Baja California peninsula, indicating that the pressure changes associated with the surge are not confined to the immediate Gulf of California environment. This might be ascribed to limited resolution of the topography by the NCEP reanalyses, but the discussion of observations below suggests the feature may be real. The extension of the negative pressure anomaly far to the south of Baja California, especially on the day of the surge, suggests a possible relationship to tropical storms passing to the south of Baja California. This will become more apparent from the upper-air analyses discussed in section 5b.

Figure 10a displays the change in surface pressure at each radiosonde station, from 1 day before to 1 day after the surge passage at Empalme. Naturally, the greatest change is at Empalme, but Mazatlan shows nearly as large a change. Changes at Tucson and Manzanillo lie along the NW–SE trending axis of greatest pressure change. Only small changes are evident away from this axis. The corresponding map of surface pressure change using the NCEP reanalysis for 1 day before and 1 day after the surge is shown in Fig. 10b. In general terms the patterns are quite similar, though the radiosonde-site-based analyses suggest a narrower band of pressure change oriented along the Gulf of California. This might be expected, possibly because the NCEP reanalysis do not resolve the topography of the region well.

Another means of displaying the pressure change dur-

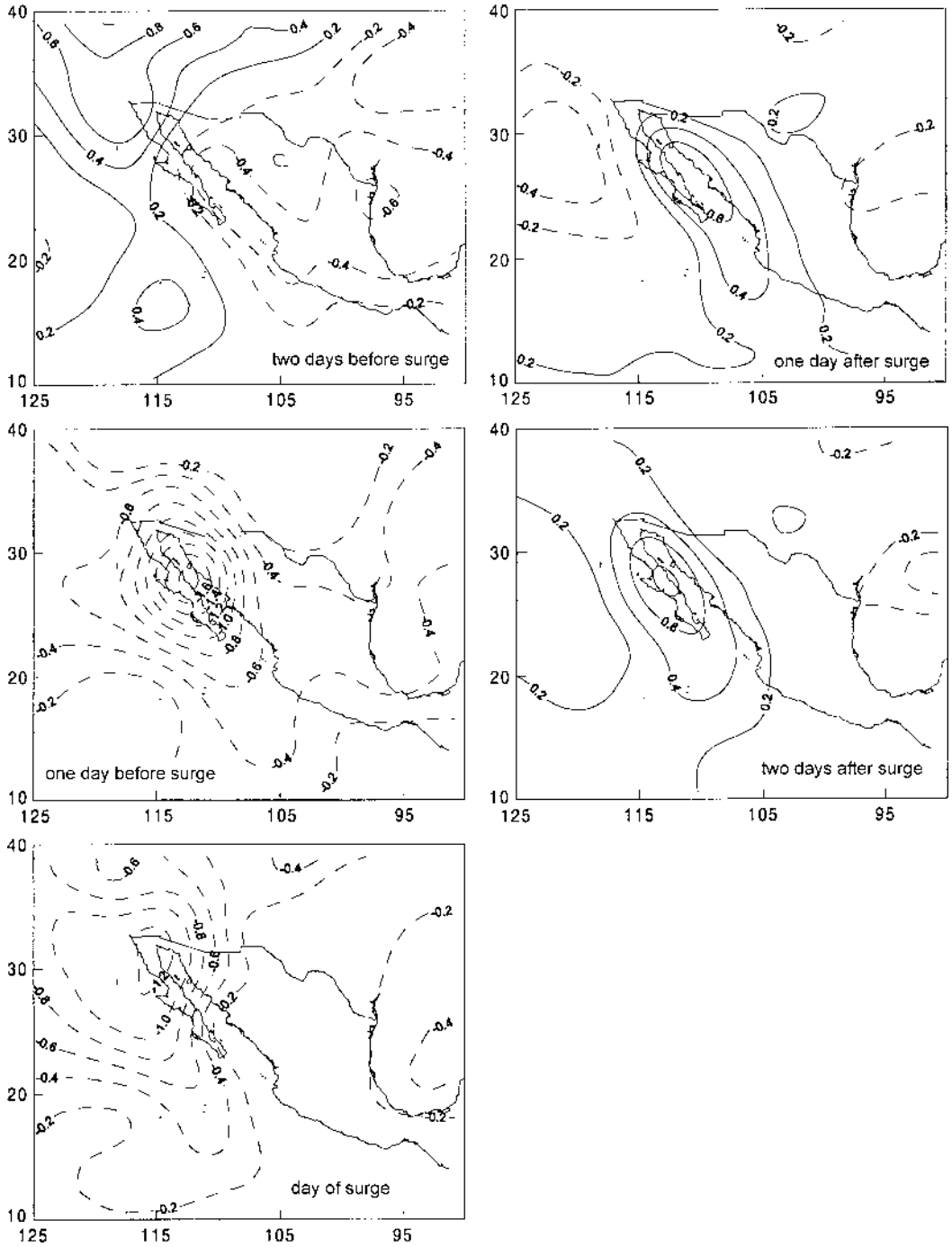

FIG. 9. Analyses of surface pressure anomalies (from Jul–Aug 8-yr means) based on the NCEP reanalysis surface pressure anomalies (see text for anomaly calculation). Contour interval 0.2 hPa; solid contours are positive anomalies, dashed are negative.

ing the surge is to calculate the magnitude of the largest pressure change during the composite surge event (defined as the maximum minus minimum pressure anomaly observed at each station during the period encompassing the surge composites). This provides a better depiction of the geographical region affected by the surge event (Fig. 10c). The main difference between Figs. 10a and 10c is that large pressure changes are now seen at Guadalupe Island and at sites in coastal southern California, well west of the mountain axis of Baja California and southern California. These pressure changes are nearly as large as those at Empalme.

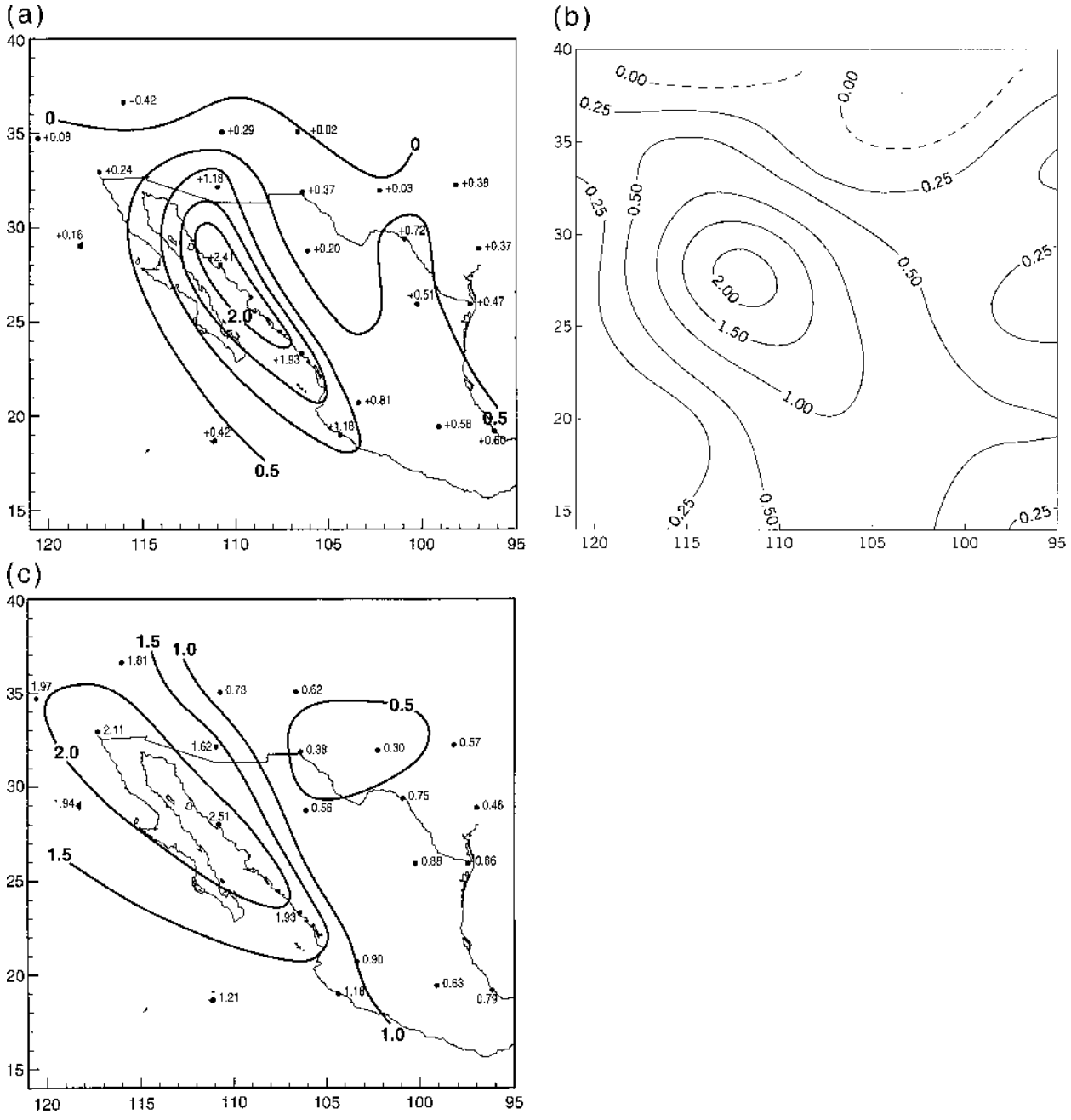

FIG. 10. Analysis of change in composite-mean surface pressure during surge passage. Contour interval is 0.5 hPa. (a) Analysis of pressure change between day before surge and day after surge passage at Empalme using radiosonde station surface pressure data, (b) same as in (a) except using only the NCEP reanalysis data, and (c) analysis of maximum pressure difference at each radiosonde site during the surge period. Note that some values are the same in (a) and (c).

b. Upper-air evolution from radiosonde observations

Radiosonde observations from central California east to west Texas and south to southern Mexico were used to produce surge composites with daily temporal resolution (Figs. 11–13). These provide a model-independent assessment of the surge structure. Examination of the different levels revealed that most of the changes can be described by considering three levels: 925, 600, and 200 hPa. The 925-hPa level, although below ground at many stations, was selected because it is near the level of maximum amplitude of the surge. The 600-hPa level was nearly halfway between 925 and 200 hPa, and showed patterns very similar to those at 700 and 500 hPa. The 200-hPa level was chosen to represent the

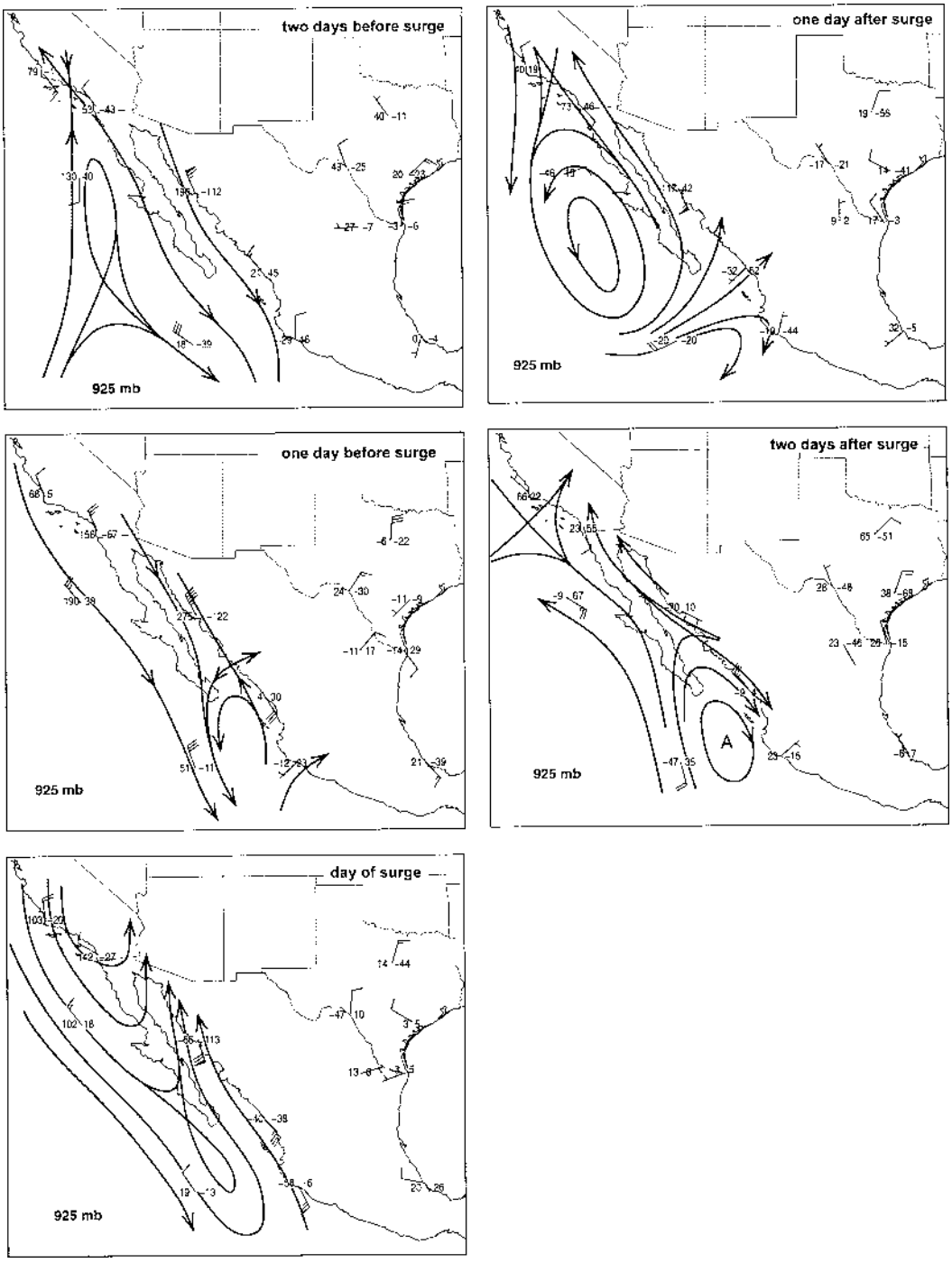

FIG. 11. Anomaly streamline analyses at 925 hPa based on radiosonde data composited with respect to the surge date at Empalme. The plotting convention is one full shaft is 0.5 m s^{-1} and one flag is 2.5 ms^{-1}. Numbers to the left of station are temperature anomalies (from long-term mean) in hundredths of °C, numbers to right are specific humidity anomalies (from long-term mean) in hundredths of gm kg^{-1}. Only winds (streamlines) are analyzed.

upper-tropospheric conditions. As with the surface pressure observations, upper-level wind, temperature, and moisture anomalies have been computed with respect to the 9 yr of July/August data to better show the spatial patterns and changes with time. As the mean vertical shear pattern is removed, anomaly fields tend to show the vertical coherence of the transient features much better.

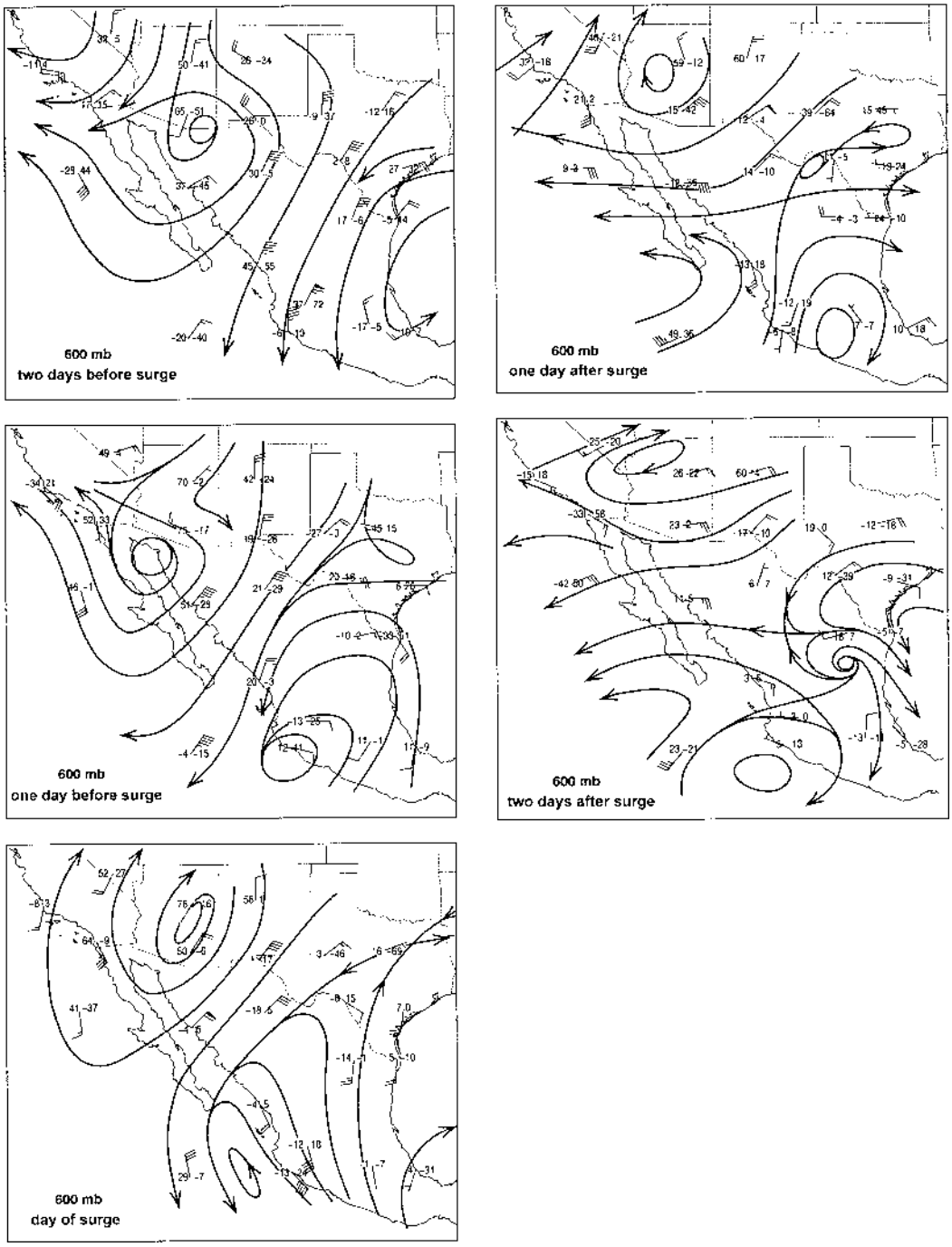

FIG. 12. Same as in Fig. 11 except at 600 hPa.

1) 925 HPA

(a) Wind anomalies

As would be expected from the compositing procedure the changes at 925 hPa (Fig. 11) are largest at Empalme, where the change in along-gulf flow is ~6.5 m s^{-1}. However, clear wind shifts from a northwesterly wind anomaly to a southeasterly anomaly are seen at all of the stations west of the continental divide, including Guadalupe Island and San Diego. The implication of this is that the gulf surge, at least the feature displayed by these composites, is not of the same horizontal scale as the cold-air outflows of isolated, or even mesoscale, convective storms. The wind anomalies have a latitudinal extent of at least 15° (San Diego to Socorro Island).

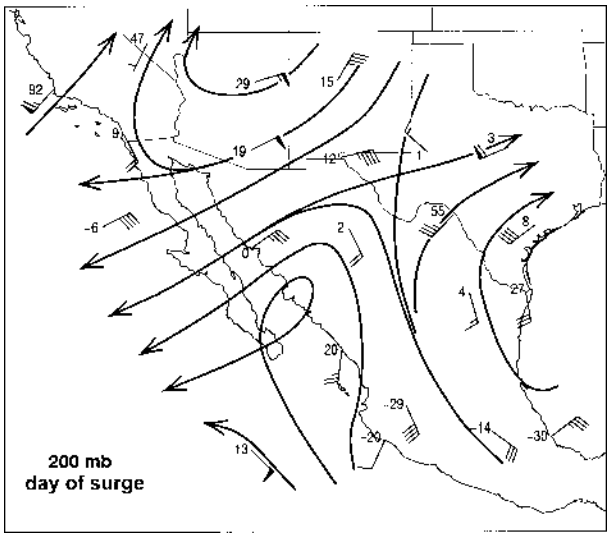

FIG. 13. Same as in Fig. 11 except at 200 hPa and only for the day of the surge passage at Empalme, and with no specific humidity anomalies shown.

Other changes that occur during the surge evolution include 1) the change from a cyclonic vorticity anomaly south of the Gulf of California to an anticyclonic anomaly after surge passage, 2) the reversal of the wind anomaly along the Gulf of California from down-gulf to up-gulf after surge passage, and 3) relatively small changes east of the Mexican plateau, over Texas and eastern Mexico.

Point 1 can be easily visualized by considering the triangle formed by the stations at Mazatlan, Socorro Island, and Manzanillo. Although cyclonic shear is evident 2 days before surge passage, it is a maximum between 1 day before and the day of the surge. Thereafter the shear weakens and the flow displays clear anticyclonic shear and curvature by 2 days after surge passage. The Mazatlan wind shift after surge passage is particularly telling. The southeast wind anomaly decreases to near zero by day T_{0+1} and becomes markedly northwesterly by T_{0+2}. This is consistent with the large positive surface pressure anomalies that develop over the central gulf late in the surge (day T_{0+2}, Fig. 9).

Point 2 highlights the strong role of the topography in dictating the wind anomalies along the gulf. The Sierra Madre Occidental barrier, extending to ~750 hPa, effectively forces the anomalies at this level to be parallel to the barrier and, thus, to the gulf. Another feature of interest is that 1 day before the surge passage at Empalme the wind has already shifted to a southeasterly anomaly at Mazatlan—indicating that surges, at least many of them, may originate south of Mazatlan. The Mazatlan anomaly has virtually the same amplitude and direction on the day T_0, indicating homogeneity after the surge passage. The same is seen at Empalme, only on days T_0 and T_{0+1}.

Point 3 suggests that far from the Gulf of California there is little signal of the surge. While this appears true at 925 hPa, it will be seen that this is not true at higher levels.

(b) Temperature and humidity anomalies

The temperature anomaly evolution at 925 hPa mirrors to a certain extent the surface pressure anomaly evolution (Fig. 9). Before the surge passage there are positive temperature anomalies over northwestern Mexico and the southwestern United States. The locus of maximum positive anomalies migrates northwestward as the surge evolves, to be replaced by a cool anomaly, with maximum negative values at Empalme 1 day after surge passage. The temperature changes are largest at Empalme, though the changes at San Diego and Guadalupe Island are about 50% that at Empalme. Most notable is the difference in temperature evolution between Empalme and Mazatlan. The change at Empalme during the surge passage (3.9°C) is more than 6 times that at Mazatlan (0.6°C), suggesting that Empalme lies closer to the mean position of the strongest thermal gradient at this level, and that wind field perturbations induce larger temperature and humidity fluctuations over the northern and central gulf than farther south. The humidity fluctuations are likewise larger at Empalme (~2.3 gm kg^{-1}) than at Mazatlan (0.9 gm kg^{-1}). Although presurge conditions at Empalme show anomalously warm and dry air being advected from the northwest, and cooler but moister conditions after surge passage, the presurge conditions at Mazatlan are actually moister, with specific humidity decreasing throughout the surge evolution. Thus, there is a slightly cooler, but drier boundary layer at Mazatlan after surge passage.

2) 600 HPA

(a) Wind anomaly evolution

The evolution of the surge wind field at 600 hPa (Fig. 12) is characterized by three main features: 1) the northwestward movement of an anticyclonic anomaly from northwestern Mexico to northern Arizona during the surge evolution, 2) the progression of a cyclonic circulation anomaly across central Mexico and its passage across the southern Gulf of California and into the tropical Pacific south of Baja California, and 3) the development, and then nearly stationary presence, of a SW–NE-oriented region of cyclonic curvature (''trough'') across north-central Mexico and west Texas (between the stations of Monterrey and Chihuahua).

The above characteristics are, of course, not necessarily independent. It is clear that a westward-moving cyclonic circulation anomaly moves from over the Gulf of Mexico and or southern Mexico, across Mexico, and into the eastern Pacific. Given that cyclonic circulations at 600 hPa are suggested near 90° and 120°W in Fig. 12, there is an implied zonal wavelength of ~30° longitude at 25°N (~3000 km). However, steady westward

translation of this wave appears to occur only south of about Mazatlan or the southern tip of the Baja California peninsula. Farther north the westward progression of the trough decelerates with time. No westward propagation is evident in the several days following the surge. In fact, the entire trough becomes more diffuse and the orientation more zonal.

Comparison of Figs. 11 and 12 shows that the wind shift from northeast to southeast at both Empalme and Mazatlan occurs 1 day after each station shifts at the 925-hPa level, in agreement with the time–height sections shown in section 4. When comparing the wind anomaly at 925 and 600 hPa over the Gulf of California, after the surge passage warm advection is evident before surge passage (veering of the wind with height) and cold advection (backing of the wind) after the surge passage. These changes are largest at Empalme, and the vertical shear is largest on the day of the surge.

(b) Temperature and humidity anomalies

The temperature anomalies at 600 hPa are much smaller than at 925 hPa, which is a reflection of the mean conditions that show lower horizontal contrast near this level (Douglas et al. 1993). The change at Empalme is about 0.6°C. Presurge conditions are generally warmer over the southwestern United States and northwestern Mexico than postsurge conditions.

Specific humidity changes are largest at stations west of the Sierra Madre Occidental, with the day before to day after surge changes largest at Tucson and Empalme in the north to Socorro Island in the south.

3) 200 HPA

In general terms the most apparent changes in the upper troposphere can be summarized as an increase in the easterly wind component over the southern United States, an increase in the westerly component over northern and central Mexico, and relatively small change over southern Mexico. However, because the analyses at 200 hPa based on the radiosonde data are similar to those from the NCEP reanalysis data, only the 200-hPa analysis on the day of the surge is shown here (Fig. 13). The main feature at 200 hPa is the trough axis extending from west Texas through the southern tip of Baja California. Lesser features, but of interest, are the composite mean winds at Mazatlan, Manzanillo, and Socorro Island, which form a triangle that can be used to estimate the vorticity. Comparison with Fig. 12 on the surge day shows this triangle to possess a cyclonic vorticity anomaly, while Fig. 13 suggests anticyclonic vorticity (mostly due to shear vorticity rather than curvature) at 200 hPa. From the thermal wind relationship this implies a relatively warm 600–200-hPa layer, which was apparent in the time section of temperature anomaly from Socorro Island (Fig. 8).

c. Surge structure and evolution from NCEP reanalyses

Because of the relatively coarse resolution of the global model used to produce the NCEP reanalyses (Kalnay et al. 1996) it was initially anticipated that the gulf surge phenomenon would be poorly depicted. The reanalysis topography does not even resolve the Baja California peninsula or the Gulf of California, both of which, from previous work, might be considered important to surge propagation. However, the results of the reanalysis-based composites discussed below are remarkably similar to those based on the radiosonde data only. In one sense this should be expected, as the radiosonde data are the primary input into tropospheric analyses during the 1980s over much of this area. We discuss the areas of agreement first, followed by some areas where discrepancies between the two analyses are evident.

Both the NCEP-based composites and the observations at 925 hPa show clear evidence of a westward-propagating tropical wave. The NW–SE trend to the trough axis orientation is especially apparent in the NCEP analyses (Fig. 14) while the observations (Fig. 11) only clearly show this orientation on the day of the surge. The horizontal extent of the northwesterly wind anomalies prior to surge passage is evident in the NCEP analyses, extending from the northern Gulf of California to south and east of Socorro Island. On the last day of the evolution sequence a cyclonic circulation is evident over the Gulf of Mexico.

Although the westward translation is similar to the propagation speed of tropical storms over this part of the eastern Pacific, the positions of the circulation centers at 925 hPa suggested in Fig. 14 are 500–800 km farther north than the average storm positions (see Fig. 18).

One difference between the two 925-hPa analyses is the intensity of the wind changes at Empalme. The radiosonde-based composites indicate a change between 2 days before and the day of the surge of ~ 7 m s^{-1}, whereas the NCEP-based analyses show a smaller change of ~ 3.5 m s^{-1}.

At 600 hPa (Fig. 15) the NCEP analyses confirm the suggestion made by the observations (Fig. 12) of a cyclonic circulation over the Gulf of Mexico 2 days before surge passage. The circulation center progresses rapidly (7°–8° longitude day^{-1}, ~ 8 m s^{-1}) westward across Mexico, then the translation slows during the last 2 days. The analyses show a large meridional extent to the trough—from less than 10°N to somewhat north of 30°N. Prior to the surge passage at Empalme, northwestern Mexico including Baja California is dominated by an anomalous ridge while the trough lies over the Gulf of Mexico and southeastern Mexico. Far to the west of Baja California a cyclonic vortex is evident; this weakens and disappears by the day of the surge. At lower latitudes the ridge preceding the surge advances

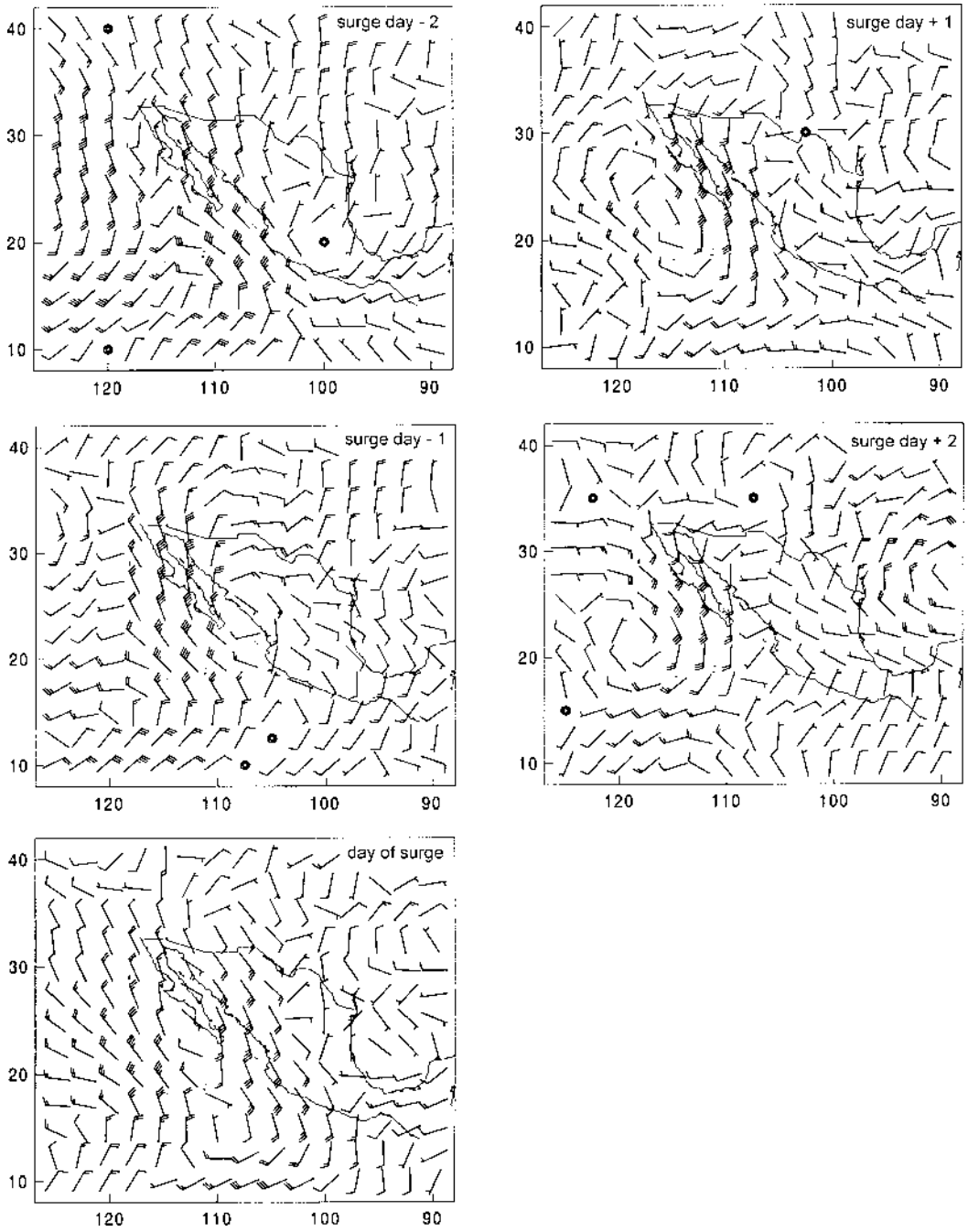

FIG. 14. Winds at 925 hPa from the NCEP reanalyses, composited with respect to surge passage at Empalme. Full shaft is 0.5 m s^{-1}; flag is 2.5 m s^{-1}.

westward and is replaced by the trough 1 day after the surge. There is little change in the position of the anomalous ridge over southern California and southwestern Arizona during the surge evolution, and north of ~35°N the ridge axis clearly shifts eastward with time. As seen at 925 hPa, by the end of the sequence (day T_{0+2}) a cyclonic circulation is evident again in the Gulf of Mexico and a prominent ridge lies across southwestern Mexico and extends off into the eastern Pacific. This is close to the position of the ridge on day T_{0-2}.

The strongest anomalous winds over the central Gulf of California are found in advance of the trough axis, prior to and on the day of the surge passage at Empalme. Weaker anomalous southwesterly flow is observed over the lower Gulf of California on the last 2 days, after passage of the trough axis.

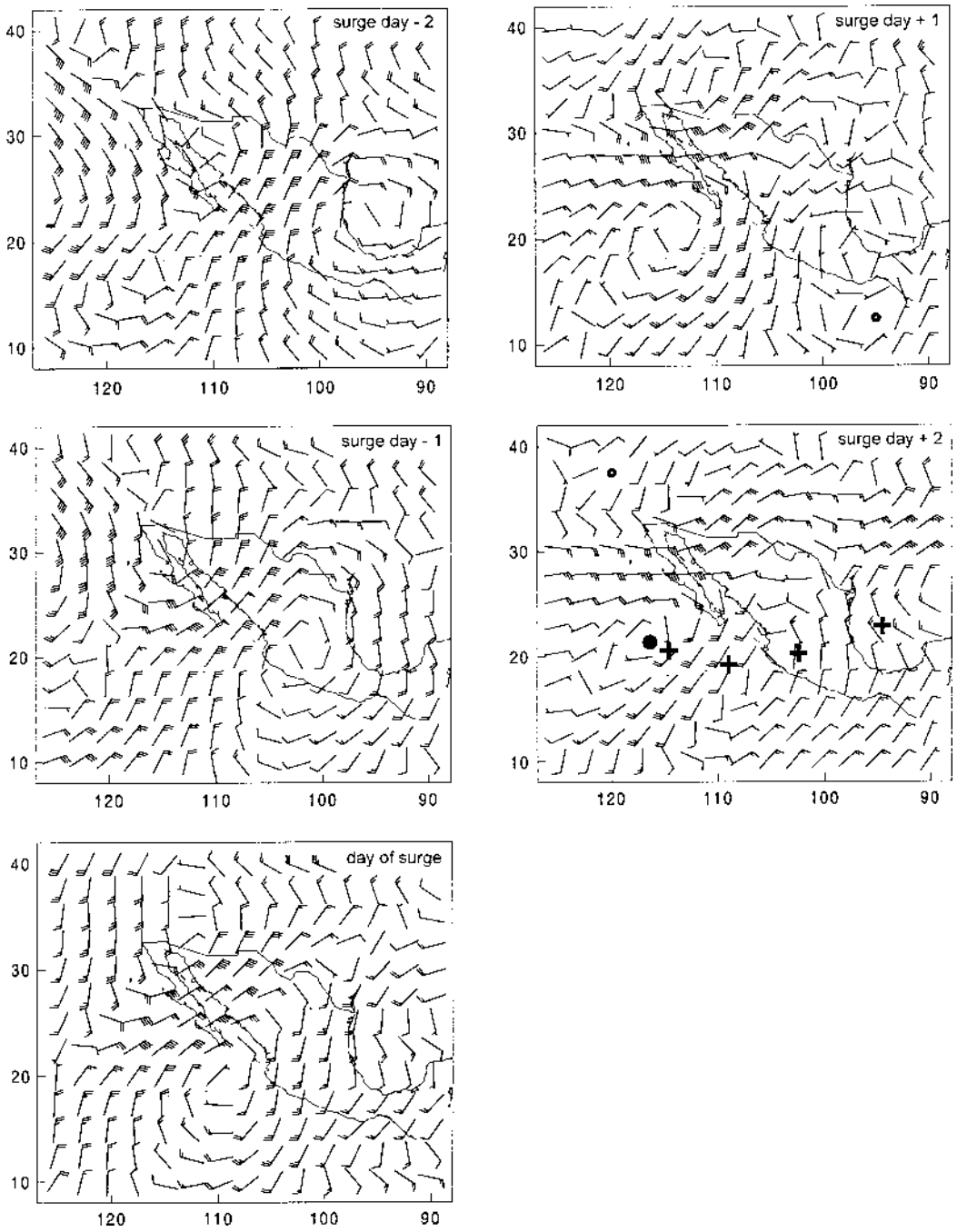

FIG. 15. Same as in Fig. 14 except at 600 hPa. Plus signs on last day [(e)] are positions of cyclonic circulation centers on previous days. Solid dot is position on last day.

In summary, the 600-hPa NCEP reanalyses provide strong evidence that gulf surges are associated with westward-propagating synoptic-scale waves that have their largest amplitude between 15° and 25°N and have their origins to the east of central Mexico. Although these waves appear to be similar in horizontal scale and propagation speed to tropical waves well documented from Atlantic field experiments (e.g., Reed et al. 1977), they occur at a slightly higher latitude. The main tropical storm path over the eastern Pacific is to the south of Mexico, near 15°–18°N along 100°–120°W. The reason for this difference in latitudinal position of the vortex track (~several hundred kilometers depending on the day of the composite) may be due to underestimation of tropical cyclone intensities in the NCEP reanalyses. Alternatively, the composite vortex may represent

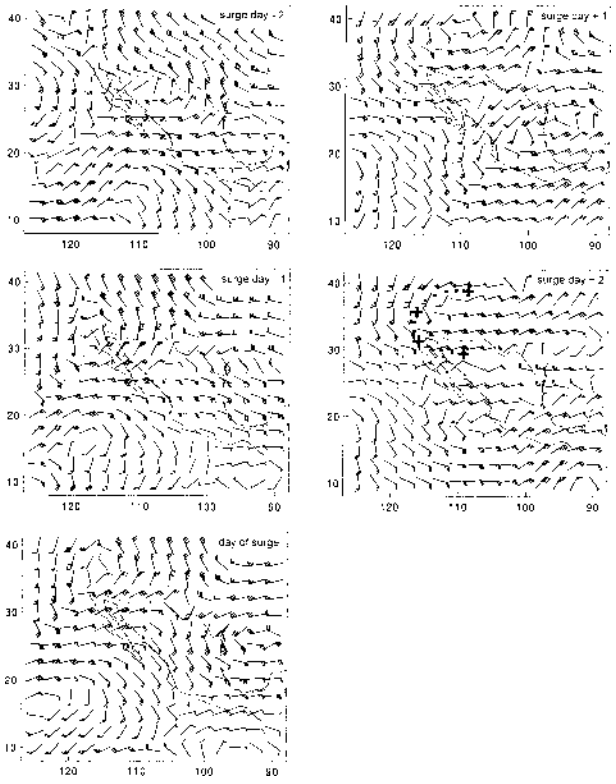

FIG. 16. Same as in Fig. 14 except at 200 hPa. Plus signs indicate positions of anticyclonic circulation center during previous days; small solid dots suggest track.

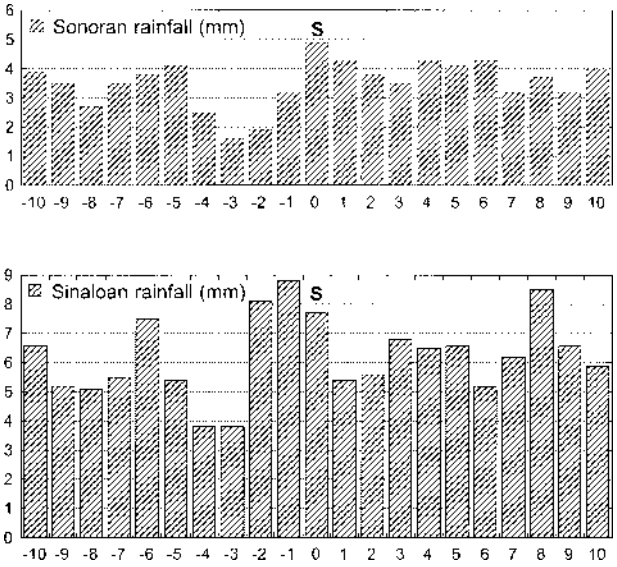

FIG. 17. Mean rainfall (mm day^{-1}) with respect to surge passage at Empalme (denoted by S) for stations in Sonora and Sinaloa. Horizontal axis is day with respect to surge onset at Empalme.

events that are associated with both tropical cyclones southwest of Mexico and subtropical voticies that are moving westward across central Mexico.

At 200 hPa (Fig. 16) the key changes during the surge passage are the weakening of the ridge axis extending from California southeastward along the U.S.–Mexico border into the Gulf of Mexico and its replacement with a SW–NE-oriented trough axis extending from the Pacific Ocean west of Baja California to southern Texas and the northern coast of the Gulf of Mexico. This is associated with the amplification of the anticyclone over the Gulf of Mexico and its southwestward extension into the eastern Pacific and the simultaneous extension of the anticyclone initially over NW Mexico, northward to almost 40°N by the end of the period.

6. Surges and rainfall over northwestern Mexico

Early studies of gulf surges were motivated by the apparent connection between surges and severe desert thunderstorms (Hales 1972; Brenner 1974). However the relationship between gulf surges and the amount of rainfall over the gulf region and surrounding desert areas has not been fully resolved. In this section we describe composites of rainfall with respect to surge onset.

While no rainfall data exists over the Gulf of California, there is a substantial body of rainfall data from the Mexican climatological network (Instituto Mexicano de Tecnología del Agua 1999). Using these data introduces some uncertainties into the comparison with the timing of surges. The rainfall from the climatological stations is measured at ~0800 local time, or about 1500 UTC. The surge passage times are defined as the first sounding that shows the evidence of the surge at 1200 UTC. Although there is probably a 12–24-h uncertainty in the timing of the surges and the rainfall, any link between rainfall and surge dates on a synoptic timescale should be evident, if one exists. Using rainfall data from available stations for the surge dates (Fig. 4) the daily mean rainfall with respect to the surge onset was calculated for the states of Sinaloa and Sonora (Fig. 17). These means are based on data from approximately 60 stations in each state. Although this is a very coarse geographical division (see Fig. 1), it suggests that surges are associated with variations in statewide rainfall. In Sinaloa there is an apparent enhancement in the rainfall 1–2 days ahead of the surge passage at Empalme, while in Sonora the highest rainfall coincides with the surge arrival at Empalme. These observations, at least conceptually, agree with the idea that surges are associated with the presence of convective cloud masses over the southern gulf, and that these in some manner develop northward with time.

It is perhaps important to note that, from Fig. 17, the actual enhancement in rainfall associated with the surge passage is not particularly large, somewhere around 15%–30% compared with values well before and well after surge passage. It is actually the presurge dryness that appears to stand out compared with the climatological daily precipitation values. The clearest evidence of this is the change from presurge dryness to postsurge

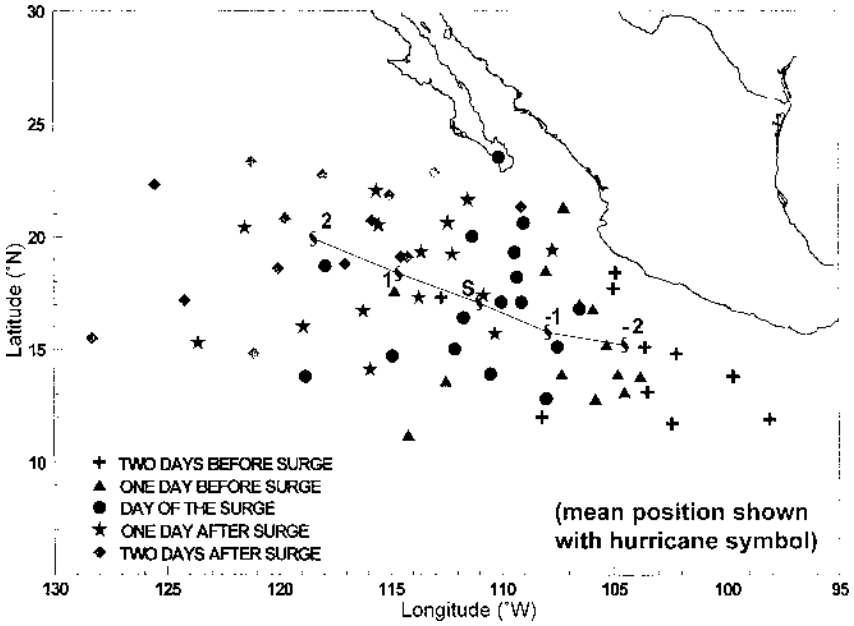

FIG. 18. Positions of individual tropical storms and hurricanes in the eastern Pacific Ocean that occurred during the surge dates used in this study. Solid plus signs are 2 days before surge at Empalme, triangles are 1 day before, dots are day of surge positions, stars are 1 day after surge, and diamond symbols are positions 2 days after surge passage. Mean positions of the positions on each date are shown by ''hurricane symbols'' connected by the solid lines.

wetness; for both Sonora and Sinaloa the precipitation roughly doubles between presurge dry days and surge wet days. Although the results here indicate that a relationship exists between surges and rainfall along the eastern side of the Gulf of California, such a relationship does not overwhelm the processes responsive for the daily precipitation patterns, at least when averaged over regions the size of these states. However, the relative contribution of surges to the mean summer rainfall may vary across Sonora and Sinaloa, as there is a large gradient in rainfall between the dry coastal areas and wetter mountains.

7. Relationship of surges with hurricanes and tropical storms

Since the results presented in section 5 suggest that surges at Empalme have a strong link with westward-propagating tropical disturbances, it is a straightforward task to see whether observed tropical storms and hurricanes cluster preferentially in certain orientations during surge occurrences. The positions of all tropical storms or hurricanes in the eastern Pacific for the July/August 1980–88 period were obtained from the Web-accessible archive of the National Hurricane Center in Miami (ftp://ftp.nhc.noaa.gov/pub/tracks/tracks.epa). These positions were then stratified by the dates of the surges at Empalme and plotted (Fig. 18). Not all storm positions are shown in Fig. 18; those storms that were clearly too far removed from the region, for example storms that were west of 120°W 2 days prior to a surge passage or east of 105°W 2 days after the surge passage, were eliminated. However, such storm positions may have entered the composite database for previous or following surges. In addition, this procedure does not guarantee that each surge is associated with a storm. For example, during the day of the surge there are only 16 positions shown in Fig. 18. This is less than half the 38 surges entering the composite. It is apparent that surges can also be associated with tropical systems that are weaker than tropical or can be unrelated to tropical storms.

Evident from Fig. 18 is the rate of propagation of the mean position of the tropical storms/hurricanes. This should be compared with the motion of the 925- and 600-hPa circulation centers in the reanalysis-based composites (Figs. 14 and 15). Although the mean storm positions and westward propagation velocities do not agree prior to the surge onset, the agreement is much better during the last 2 days of the sequence when the mean position of the storms and the 600 hPa center is very close.

8. Summary

The gulf surge phenomenon has been described in the scientific literature for approximately 30 years. Despite this, few studies have used a compositing procedure similar to that used in the present study to describe surge characteristics. The procedure employed was straightforward: to identify the surge passages during July and August at Empalme, Sonora, over a 9-yr period

(selected for its data completeness) and then composite the available historical radiosonde data with respect to the dates of surge passage. Although the identification of a gulf surge from only one station continues to present uncertainties, the results presented in this study seem to justify both the procedure and the selection of surge dates chosen for compositing.

The compositing procedure has revealed the mean surge characteristics (vertical structure of the temperature, moisture, and wind anomalies) at Empalme. This showed that the largest changes during surges are near 950 hPa, that the warm air anomaly ahead of surges is a larger departure from climatology than the cool air anomaly after surges, and that the surges tilted southward with height. Surges at Empalme are related to the passage of synoptic-scale circulation features in the lower–middle troposphere, most clearly seen near the 600-hPa level. This composite cyclonic circulation feature can be traced upstream to over the Gulf of Mexico 2 days prior to the surge passage at Empalme. However, this conclusion is valid only so long as the compositing assumption is valid—that most surges are similar.

This study has also shown that surges are related to the position of tropical storms and hurricanes over the eastern Pacific Ocean. On the day of surge onset at Empalme the mean position of eastern Pacific storms and hurricanes was ~300–500 km south of the southern tip of the Baja California peninsula. However, since the number of surges was more than the number of storm positions, not all surges have a clear relationship with storms. This suggests that multiple mechanisms are responsible for surges. We have not made an attempt to identify the mechanism relating surges to storms in this study, only to see whether a preferred geographical position is evident.

Finally, rainfall over the eastern side of the Gulf of California is modulated by surges, though the effect is modest. The character of this rainfall modulation changes along the gulf, with rain over the southern state of Sinaloa occurring prior to the surge passage at Empalme, while rainfall occurs on the same day or just after surge passage over the northern state of Sonora. This is consistent with the notion that surge initiation is associated with widespread convection at the southern end of the Gulf of California, and that this convection propagates northward as suggested in the first studies by Hales (1972) and Brenner (1974). However, cause and effect is not established by the present study.

Although indicating that surges modulate rainfall over northwest Mexico, this study has not explored the geographical rainfall variations in detail. It may be that the rainfall modulation is relatively large along the coastal plain, and low along the foothills of the Sierra Madre Occidental—or the reverse. Likewise, although modest in overall contribution when averaged over an entire state, it may be that the rainfall contribution of surges to the driest parts of the Sonoran Desert is more significant than suggested here. Stratification by smaller geographical regions would be necessary to answer these questions, though the climatological database will ultimately limit the details that can be discerned. Satellite imagery could be used productively to produce a composite evolution of the surge event, using the surges dates of this study. Such a dataset was not available to the authors, but presumably could be exploited to complement strictly rainfall-based studies of the surge impact.

Acknowledgments. Some of the work reported here formed part of the M.S. thesis of JCL at the Centro de Investigacion Cientifica y Estudios Superiores de Ensenada (CICESE), Mexico. JCL wishes to thank the Consejo Nacional de Ciencias y Tecnologia (CONACyT) of Mexico for supporting his studies while at CICESE and for the guidance provided by members of his committee, consisting of Drs. Maria Luisa Argote, Antonio Badan-Dangon, Gilberto Gaxiola, and Edgar Pavia. An extended stay at NSSL, during which many other aspects of this study were carried out, was sponsored by the NOAA Office of Global Programs as part of the PACS-SONET project. Help with dataset manipulation that was provided by Javier Murillo, Jose Meitin, and Malaquias Peña was much appreciated. Valuable comments on an earlier draft were provided by Bob Maddox and Dave Stensrud of NSSL.

REFERENCES

Adams, D. K., and A. C. Comrie, 1997: The North American Monsoon. *Bulletin Amer. Meteor. Soc.,* **78,** 2197–2213.

Anderson, B. T., J. O. Roads, and S. C. Chen, 2000a: Large-scale forcing of summertime monsoon surges over the Gulf of California and the southwestern United States. *J. Geophys. Res.,* **105** (D19), 24 455–24 467.

——, ——, ——, and H.-M. H. Juang, 2000b: Regional simulation of the low-level monsoon winds over the Gulf of California and southwestern United States. *J. Geophys. Res.,* **105** (D14), 17 955–17 969.

Anthes, R. A., 1982: *Tropical Cyclones.* Amer. Meteor. Soc., 208 pp.

Brenner, I. S., 1974: A surge of maritime tropical air-Gulf of California to the Southwestern United States. *Mon. Wea. Rev.,* **102,** 375–389.

Djuric, D., 1994: *Weather Analysis.* Prentice Hall, 304 pp.

Douglas, M. W., 1995: The summertime low-level jet over the Gulf of California. *Mon. Wea. Rev.,* **123,** 2334–2347.

——, and S. Li, 1996: Diurnal variation of the lower-tropospheric flow over the Arizona low desert from SWAMP-1993 observations. *Mon. Wea. Rev.,* **124,** 1211–1224.

——, R. A. Maddox, K. Howard, and S. Reyes, 1993: The Mexican monsoon. *J. Climate.,* **6,** 1665–1677.

Hales, J. E., Jr., 1972: Surges of maritime tropical air northward over the Gulf of California. *Mon. Wea. Rev.,* **100,** 298–306.

Fuller, R. D., and D. J. Stensrud, 2000: The relationship between easterly waves and surges over the Gulf of California during the North American monsoon. *Mon. Wea. Rev.,* **128,** 2983–2989.

Instituto Mexicano de Tecnología del Agua, 1999: ERIC: Extractor Rápido de Informacion Climatológica. CD-ROM. [Available from Instituto Mexicano de Tecnología del Agua, Paseo Cuauhnáhuac 8532, Juitepec, Morelos, México.]

Kalnay, E., and Coauthors, 1996: The NCEP/NCAR 40-Year Reanalysis Project. *Bull. Amer. Meteor. Soc.,* **77,** 437–471.

?5

Meitin, J. G., K. W. Howard, and R. A. Maddox, 1991: Southwest area monsoon project. Daily operations summary. [Available from National Severe Storms Laboratory, Norman, OK. 73069.]

Press, W. H., B. P. Flannery, S. A. Teukolsky, and W. T. Vetterling, 1986: *Numerical Recipes: The Art of Scientific Computing.* ??? pp.

Reed, R. J., D. C. Norquist, and E. E. Recker, 1977: The structure and properties of African wave disturbances as observed during phase III of GATE. *Mon. Wea. Rev.,* **105,** 317–333.

Reyes, S., M. W. Douglas, and R. A. Maddox, 1994: El monzón del suroeste de Norteamérica (TRAVASON/SWAMP). *Atmósfera,* **7,** 117–137.

Schmitz, J. T., and S. L. Mullen, 1996: Water vapor transport associated with the summertime North American monsoon as depicted by ECMWF analyses. *J. Climate,* **9,** 1621–1634.

Stensrud, D. J., R. L. Gall, and M. K. Nordquist, 1997: Surges over the Gulf of California during the Mexican monsoon. *Mon. Wea. Rev.,* **125,** 417–437.